Transport properties of ultra-thin VO2 films on (001) TiO2 grown by reactive molecular-beam epitaxy

Hanjong Paik, Jarrett A. Moyer, Timothy Spila, Joshua W. Tashman, Julia A. Mundy, Eugene Freeman, Nikhil Shukla, Jason M. Lapano, Roman Engel-Herbert, Willi Zander, Jürgen Schubert, David A. Muller, Suman Datta, Peter Schiffer, and Darrell G. Schlom

---

Articles you may be interested in

Visualization of local phase transition behaviors near dislocations in epitaxial VO2/TiO2 thin films
Appl. Phys. Lett. **107**, 171603 (2015); 10.1063/1.4934943

Epitaxial growth of VO2 by periodic annealing
Appl. Phys. Lett. **104**, 063104 (2014); 10.1063/1.4864404

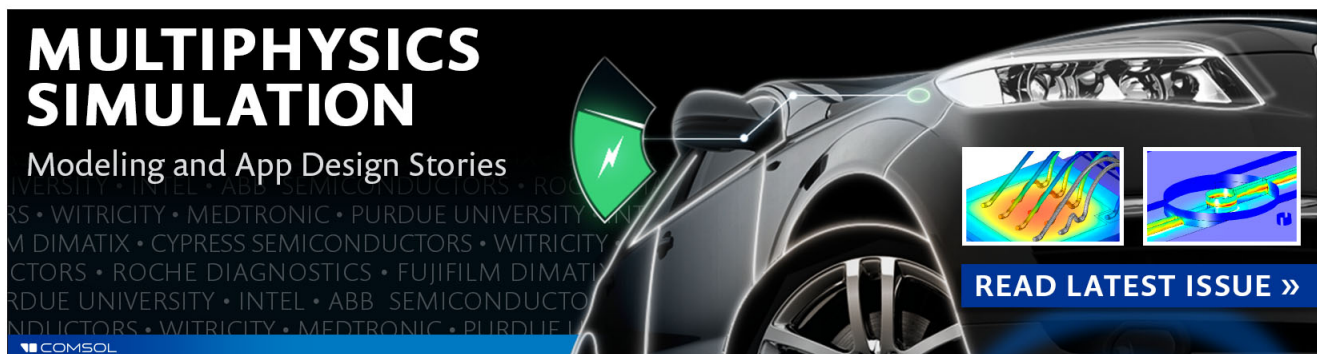Control of tensile strain and interdiffusion in Ge/Si(001) epilayers grown by molecular-beam epitaxy
J. Appl. Phys. **114**, 083504 (2013); 10.1063/1.4818945

Growth of epitaxial oxides on silicon using atomic layer deposition: Crystallization and annealing of TiO2 on SrTiO3-buffered Si(001)
J. Vac. Sci. Technol. B **30**, 04E111 (2012); 10.1116/1.4734311

C lattice site distributions in metastable Ge 1−y C y alloys grown on Ge(001) by molecular-beam epitaxy
J. Appl. Phys. **91**, 3644 (2002); 10.1063/1.1448677

Transport properties of ultra-thin VO₂ films on (001) TiO₂ grown by reactive molecular-beam epitaxy

Hanjong Paik,[1] Jarrett A. Moyer,[2,3] Timothy Spila,[3] Joshua W. Tashman,[1] Julia A. Mundy,[4] Eugene Freeman,[5] Nikhil Shukla,[5] Jason M. Lapano,[6] Roman Engel-Herbert,[6] Willi Zander,[7] Jürgen Schubert,[7] David A. Muller,[4,8] Suman Datta,[5] Peter Schiffer,[2,3] and Darrell G. Schlom[1,8,a)]

[1]Department of Material Science and Engineering, Cornell University, Ithaca, New York 14853, USA
[2]Department of Physics, University of Illinois Urbana-Champaign, Urbana, Illinois 61801, USA
[3]Materials Research Laboratory, University of Illinois Urbana-Champaign, Urbana, Illinois 61801, USA
[4]School of Applied and Engineering Physics, Cornell University, Ithaca, New York 14853, USA
[5]Department of Electrical Engineering, The Pennsylvania State University, University Park, Pennsylvania 16802, USA
[6]Department of Materials Science and Engineering, The Pennsylvania State University, University Park, Pennsylvania 16802, USA
[7]Peter Grünberg Institute (PGI9-IT), JARA-Fundamentals of Future Information Technologies, Research Centre Jülich, D-52425 Jülich, Germany
[8]Kavli Institute at Cornell for Nanoscale Science, Ithaca, New York 14853, USA

We report the growth of (001)-oriented VO₂ films as thin as 1.5 nm with abrupt and reproducible metal-insulator transitions (MIT) without a capping layer. Limitations to the growth of thinner films with sharp MITs are discussed, including the Volmer-Weber type growth mode due to the high energy of the (001) VO₂ surface. Another key limitation is interdiffusion with the (001) TiO₂ substrate, which we quantify using low angle annular dark field scanning transmission electron microscopy in conjunction with electron energy loss spectroscopy. We find that controlling island coalescence on the (001) surface and minimization of cation interdiffusion by using a low growth temperature followed by a brief anneal at higher temperature are crucial for realizing ultrathin VO₂ films with abrupt MIT behavior. © 2015 AIP Publishing LLC.
[http://dx.doi.org/10.1063/1.4932123]

Controlling the metal-to-insulator transition (MIT) of vanadium dioxide (VO₂) by means of an external electric-field, the so called the "MIT transistor" concept, has received significant recent attention.[1,2] Ionic-liquid-gating has been reported to apply a huge electric-field to the VO₂ channel, resulting in an electric-field driven metallic state throughout the entire VO₂ channel.[1] The slow response time of ionic-liquid gating due to its polarization arising from space charge and its propensity to chemically react with VO₂ and form oxygen vacancies,[2] however, make it unlikely to be practical for electronics applications.

An alternative approach to practical MIT transistors is to use a solid gate dielectric with a high dielectric constant (K),[3] but this approach requires VO₂ films that are only a few nm thick with a large relative change in resistance ($\Delta R/R$) at the MIT. In bulk single crystals of VO₂, $\Delta R/R$ is of order 10^5 (Ref. 4), but $\Delta R/R$ of 10^4 had only been achieved for VO₂ films 100 nm or more in thickness,[5–7] until recently when $\Delta R/R$ of 10^4 was reported in a 10 nm thick epitaxial VO₂ film grown on (001) TiO₂.[8,9] For thinner samples, the $\Delta R/R$ was observed to quickly degrade until no transition at all was seen in uncapped samples 3 nm or less in thickness.[8]

In this letter, we describe a method for growth of ultra-thin VO₂ films by molecular-beam epitaxy (MBE). The prior route to VO₂ films by MBE has been previously described as the "epitaxy by periodic annealing" method, in which sub-monolayer amorphous vanadium metal is deposited and subsequent annealing in distilled ozone at a relatively low growth temperature (to minimize interdiffusion).[10] Our current method for VO₂ growth by MBE is both faster and more amenable to variations in growth parameters. Using it, we achieve abrupt and reproducible MITs in VO₂ films as thin as 1.5 nm, and with large values of $\Delta R/R$. The key to this alternative growth method is the vanadium oxidation kinetics, i.e., a slow growth rate and distilled ozone are necessary to achieve an MIT in MBE-grown VO₂.

To estimate the relevant thickness of VO₂ film for a dielectric-gated MIT transistor, we calculate the Debye length (or Thomas-Fermi screening length) $L = \sqrt{\frac{\epsilon_0 K k_B T}{e^2 n_e}}$, to be in the 0.7–5.8 nm range for VO₂ in the insulating (semiconducting) state, where its critical carrier concentration, $n_e \approx 4.0 \times 10^{18}$–$9.6 \times 10^{19}$ cm^{-3} from the Mott's criteria, $n_e = \left(\frac{0.25}{\alpha_H}\right)^3$, $\alpha_H = \frac{h^2 \epsilon_0 K}{\pi m^* e^2}$, $K \approx 36$–100 (Refs. 11 and 12), ϵ_0 is the permittivity of free space, h is Plank's constant, $m^* \approx 3.5 m_e$ is the effective mass of electrons in VO₂ (Ref. 13), m_e is the mass of an electron, k_B is Boltzmann's constant, T is room temperature (300 K), and e is the charge of an electron. For VO₂ in the metallic state, this length is even shorter.

We grew epitaxial VO₂ thin films on rutile (001) TiO₂ single crystal substrates by reactive MBE in a Veeco

a)Author to whom correspondence should be addressed. Electronic mail: schlom@cornell.edu

GEN10. The vanadium flux was calibrated to be in the range of 2–3×10^{12} atoms/(cm^2·s) by a quartz crystal microbalance (QCM) before growth. This flux is an order of magnitude lower than that used in the periodic annealing method.[10] Vanadium and distilled ozone were codeposited onto the (001) TiO$_2$ substrate held at $250\,°C$ (thermocouple temperature) under a distilled ozone background pressure of 1.0×10^{-6} Torr. The resulting VO$_2$ film growth rate was about 0.012–0.015 Å/s. The optimal growth temperature (T_s) was established from MIT transport measurements (see supplementary Figure S1).[29] It should be noted that a low hydrogen partial pressure (less than 4×10^{-9} Torr) was required to achieve a sharp MIT.[14]

Following deposition of the desired film thickness, the temperature of the sample was rapidly ramped to $350\,°C$, then immediately cooled to below $100\,°C$ under the same background pressure of distilled ozone (1×10^{-6} Torr). This *in situ* flash annealing step improved the film smoothness and resulted in a more abrupt MIT (see supplementary Figure S2).[29] *In situ* reflection high-energy electron diffraction (RHEED) was used to monitor film growth. Four-circle X-ray diffraction (XRD) with a 220 Ge monochromator and a 220 Ge analyzer were used to assess the structural quality of the films at room temperature. The film thickness was estimated from the vanadium flux measured by the QCM and confirmed by the spacing of the XRD thickness fringes (Kiessig fringes) of the 002 VO$_2$ Bragg peak. The film thickness was corroborated by measuring the areal density of vanadium atoms by Rutherford backscattering spectrometry (RBS), and assuming films to have bulk VO$_2$ density.[15] Low-angle annular dark field (LAADF) scanning transmission electron microscopy (STEM) confirmed the interfacial atomic structure; electron-energy loss spectroscopy (EELS) was used to assess the vanadium valence state and to evaluate the titanium interdiffusion length. The surface morphology was characterized by atomic force microscopy (AFM). Temperature-dependent electrical transport was measured using the van der Pauw 4-point method where the sample was contacted with gold wires and silver paint.

To optimize film growth, we developed a surface termination recipe for the (001) TiO$_2$ surface by chemical etching and annealing. After rinsing in organic solvents, the substrates were etched in a 23% HF aqueous solution to remove metallic impurities from the TiO$_2$ surface. The substrates were then heated to $1050\,°C$ in air and cooled down to room temperature with dwell steps at $950\,°C$ for 30 min and at $850\,°C$ for 60 min to promote the formation of an atomically smooth, stable surface. A terminated (001) TiO$_2$ surface with a well-defined step and terrace structure was revealed directly by AFM and indirectly by RHEED (see supplementary Figure S3).[29] Note that our etching/annealing recipe for (001) TiO$_2$ only worked for single crystals grown by the floating zone method.[16] Prior to growth, the substrates were heated to $250\,°C$ in a distilled ozone background pressure of 1×10^{-6} Torr. Strong Kikuchi lines are evident on the bare (001) TiO$_2$ substrate (region α in Fig. 1), indicative of a smooth and well ordered surface.

Growth of VO$_2$ on terminated (001) TiO$_2$ substrates proceeded in a manner similar to Fig. 1; a three-dimensional transmission RHEED pattern occurred despite the surface termination of the TiO$_2$ substrate. Figure 1 shows the time dependence of the growth parameters used for a 10 nm thick VO$_2$ film deposited on (001) TiO$_2$ as well as the *in situ* RHEED pattern evolution during the growth. The α, β, γ, δ image sequence corresponds to RHEED images during VO$_2$ growth along the [110] (top row) and [100] (bottom row) azimuthal directions. VO$_2$ growth was initiated by supplying a continuous low flux of vanadium (region β). At this point, the RHEED intensity was monitored, but RHEED oscillations were not observed during growth. Instead, the growing film developed a Volmer-Weber type transmission RHEED pattern (region γ). This surface roughening originates from (001) having the highest surface energy of the low index planes of rutile.[17,18] The rough three-dimensional growth
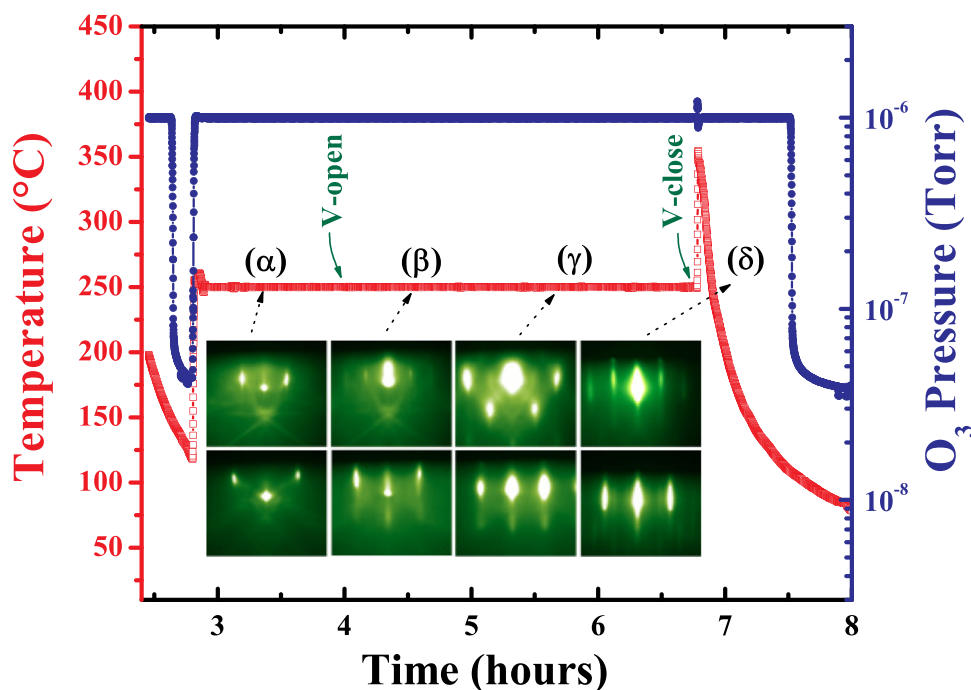

FIG. 1. Evolution of the RHEED patterns observed during the growth of a 10 nm thick epitaxial VO$_2$ thin film. RHEED images are shown during the growth along the [110] azimuth (top row) and along the [100] azimuth (bottom row) at four times. (α) Bare (001) TiO$_2$ substrate at $250\,°C$ in a 1×10^{-6} Torr background pressure of distilled ozone. (β) Initiation of VO$_2$ growth by opening the vanadium shutter. (γ) After the growth of 5 nm of VO$_2$. (δ) After flash-annealing at $350\,°C$ and cooling the film down to below $100\,°C$ in a background pressure of 1×10^{-6} Torr of distilled ozone.

nature of the (001) VO$_2$ film could be modified (region δ) after the growth was complete utilizing flash annealing to 350 °C followed immediately by cooling to below 100 °C in the same distilled ozone background pressure (1×10^{-6} Torr). This final step enhanced the coalescence of (001)-oriented VO$_2$ islands; it also improved the abruptness of the MIT (see supplementary Figure S2).[29] Annealing temperatures higher than 350 °C degraded the MIT and raised the MIT transition temperature T_c; this is likely due to the diffusion of titanium from the substrate into the VO$_2$ films.

$\theta/2\theta$ XRD patterns of VO$_2$ thin films with thicknesses ranging from 1.5 to 30 nm are shown in Fig. 2(a). Well-defined thickness fringes are seen in the thicker films, and the film thickness calculated from these fringes is consistent with the QCM flux measurement within our ±10% error bar. The normalized 002 rocking curves of VO$_2$ films are over-laid in Fig. 2(b), and the full width at half maximum (FWHM) values of the rocking curves are plotted in Fig. 2(c). The FWHM values of VO$_2$ films with thickness between 3 and 10 nm are 0.004°–0.0045°. These values are comparable to those of the 002 rocking curves of the under-lying TiO$_2$ substrates (0.004°–0.0044°), demonstrating the

similar structural quality between film and substrate. For thicker VO$_2$ films, the FWHM increases slightly to 0.006°–0.007° for the 15 and 20 nm thick films, and the structural relaxation is clearly seen in the 30 nm thick film (FWHM of 0.012°). The c-axis length of the VO$_2$ films was calculated based on a Gaussian fit to the 002 VO$_2$ peaks (Fig. 2(a)), and the a-axis length was calculated based on scans of the off-axis 101, 202, and 303 peaks and a Nelson-Riley fit[19] of the d_{101} spacing (Fig. 2(d)). The relaxation with film thickness is apparent in the FWHM of the rocking curve and the film a-axis length of films over 15 nm thick.

Figure 3(a) shows the temperature-dependent electrical transport (resistivity vs. temperature) of the same VO$_2$ films. The $\Delta R/R$, T_c, transition width, and hysteresis characteristics of the MIT were analyzed using an established method,[10] and are given in Table I. An abrupt resistivity change with $\Delta R/R \approx 10^3$ is consistently observed in films with thicknesses ranging from 3 to 20 nm. In this film thickness range, T_c resided around 290 ± 5 K with a hysteresis value of 12 ± 3 K. The lower T_c compared to bulk or single crystal-line VO$_2$ ($\sim$340 K)[4] is consistent with a biaxial in-plane ten-sile strain effect.[20] The lower T_c exhibited by the films under
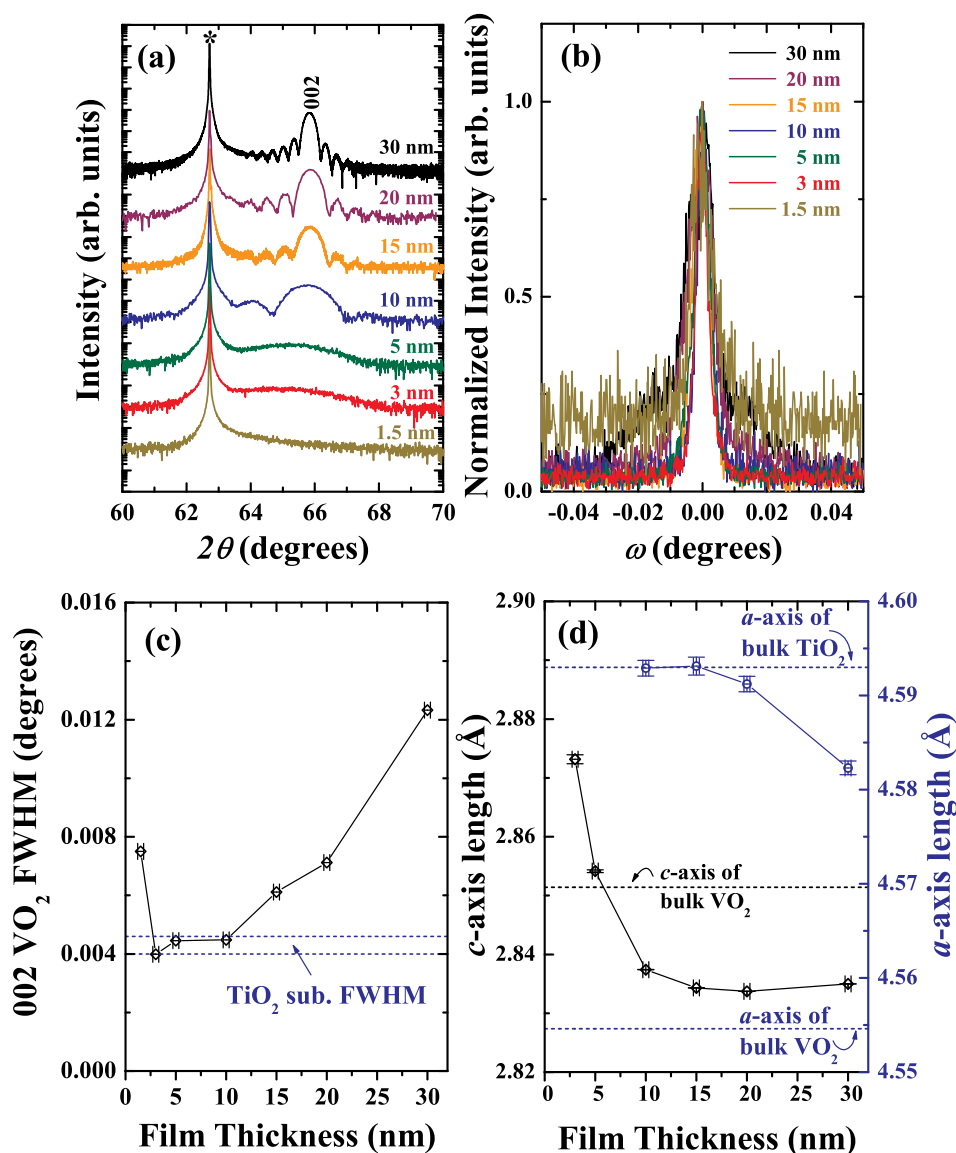

FIG. 2. (a) $\theta/2\theta$ XRD scans of VO$_2$ thin films grown on rutile (001) TiO$_2$ substrates as a function of film thick-ness ranging from 1.5 to 30 nm. The peak arising from the 002 reflection of the rutile TiO$_2$ substrate is labeled with an asterisk (*); the remaining peak (and thickness fringes) is from the 002 reflection of VO$_2$. (b) 002 Rocking curve comparison of the VO$_2$ thin films. (c) Thickness dependence of the FWHM of the rocking curve of the 002 VO$_2$ peaks. The dashed lines indicate the range in the rocking curve FWHM of the 002 TiO$_2$ peaks of the substrates upon which the VO$_2$ films were grown. (d) Thickness dependence of the out-of-plane lattice constant calculated from the $\theta/2\theta$ scans and in-plane lattice constant calculated from the (101) off-axis $\theta/2\theta$ scans.
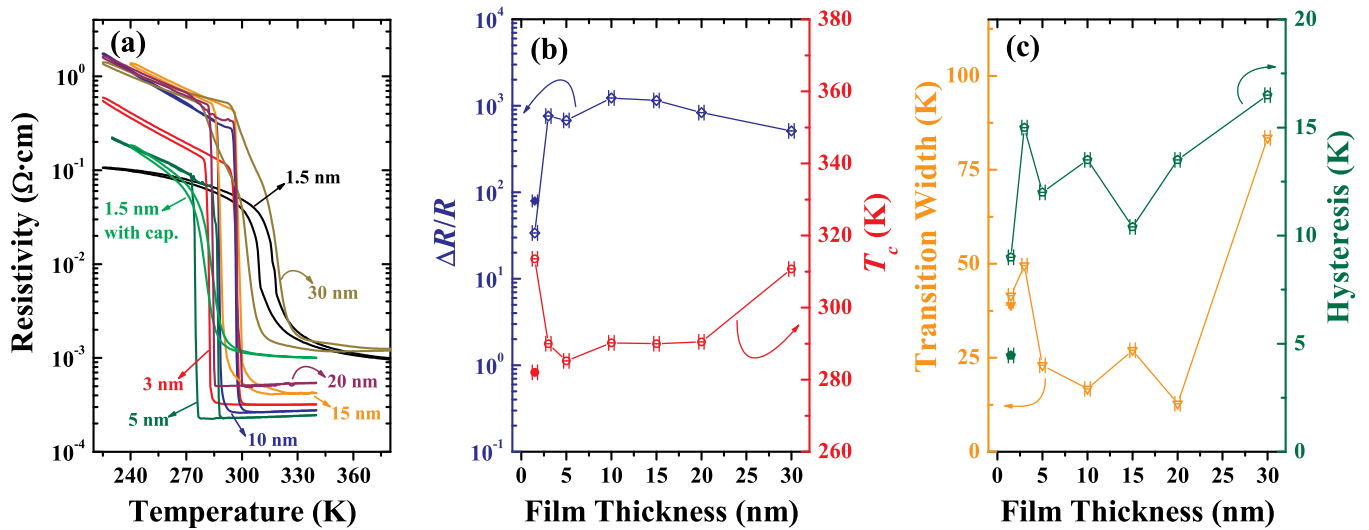
FIG. 3. (a) Resistivity vs. temperature of the same films studied in Fig. 2. The thickness dependence of the MIT transition temperature (T_c), transition width, and hysteresis are shown in (b) and (c). All quantities were determined as described in Ref. 11. The single filled symbols in Figs. 3(b) and 3(c) represent the results of the 1.5 nm thick VO$_2$ films with a 5 nm thick amorphous LaAlO$_3$ capping layer.

biaxial tensile strain results from a shortened c-axis lattice parameter, stabilizing the metallic ground state by the increase of overlap between the vanadium and oxygen atoms along the c-axis.[21] The higher resistivity observed for the 15 and 20 nm thick films in their metallic state compared to the coherently strained VO$_2$ films (between 3 and 10 nm thick VO$_2$) could be due to defects associated with film relaxation. For the 30 nm thick film, multiple steps are seen in the ρ vs. T transport behavior. This multistep MIT behavior originates from microcracks disrupting the homogeneous flow of current, as revealed by the AFM measurements in Fig. 4(a), showing the existence of such cracks in these same films. Our observation is consistent with other reports,[22] and such cracks are common in tensile strained oxide films.[23]

A suppression of the MIT (i.e., a decreased $\Delta R/R$) was observed as the VO$_2$ film thickness reached the ultra-thin 1.5 nm thickness range (without a capping layer). The observed suppression of the MIT and its slanted shape (see Fig. 3(a)) could be due to surface degradation from air exposure. To check this possibility, we deposited a 5 nm thick amorphous LaAlO$_3$ capping layer on top of the 1.5 nm VO$_2$ film before removing it from the MBE and exposing it to air. A suppressed and slanted MIT behavior was still observed, however, and the transition temperature was lower than for

the film without a capping layer. The film roughness arising from the Volmer-Weber growth mode, and resulting inhomogeneous film connectivity and current flow could be responsible for the slanted MIT behavior of the 1.5 nm VO$_2$ film. Another possible extrinsic cause of the suppression of the MIT in the ultrathin VO$_2$ films is interdiffusion with the substrate.[24]

TABLE I. MIT characteristics of the same VO$_2$ films as shown in Fig. 3 using the analysis method described in Ref. 10.

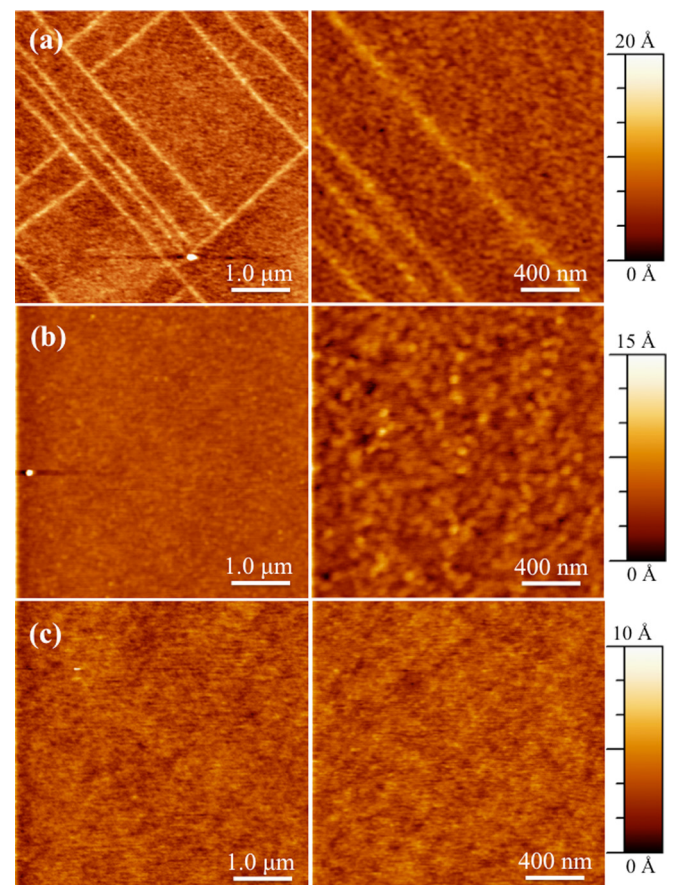| Nominal Thickness (nm)	RBS Thickness (nm)	T_c (K)	$\log_{10}(\Delta R/R)$	Transition width (K)	Hysteresis (K)
1.5 (w/o cap)	1.4 ± 0.3	313.5	1.53	41.5	9.0
1.5 (with cap)	1.6 ± 0.3	282.1	1.90	39.0	4.5
3	3.0 ± 0.3	290.0	2.88	49.5	15.0
5	4.9 ± 0.3	285.2	2.83	23.0	12.0
10	9.1 ± 0.3	291.0	3.09	16.8	9.5
15	14.7 ± 0.3	293.0	3.06	27.0	10.4
20	20.3 ± 0.3	290.5	2.90	12.8	13.5
30	29.2 ± 0.3	310.0	2.71	83.5	16.5

FIG. 4. AFM images of VO$_2$ films with thicknesses (a) 30 nm, (b) 10 nm, and (c) 3 nm. Structural and transport measurements of the same films are shown in Figs. 2 and 3.
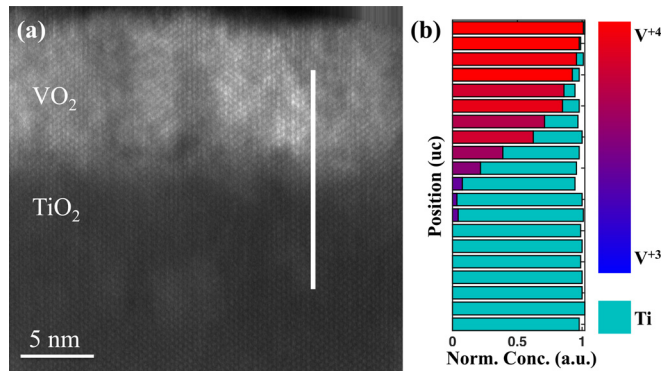
FIG. 5. (a) Cross-sectional LAADF-STEM image of a 9 nm thick epitaxial VO_2 film grown on (001) TiO_2. (b) Vanadium and titanium EELS L-edge line-scan across the film/substrate interface, showing the normalized concentrations (Norm. Conc.) of these constituents. These data indicate that the titanium and vanadium interdiffusion length is 1.4–1.7 nm and also shows a vanadium valence fluctuation at the interface.

The chemical interdiffusion between film and substrate was characterized using LAADF-STEM and EELS. Figure 5(a) shows a LAADF-STEM image of the VO_2 films; LAADF-STEM was chosen in contrast to high-angle annular dark field STEM (HAADF-STEM) due to the low Z-contrast between vanadium and titanium. The interface is coherent yet appears diffuse over approximately 1 nm. Figure 5(b) shows the corresponding EELS line profile of the vanadium and titanium concentrations acquired from the V-$L_{2,3}$ and Ti-$L_{2,3}$ edges, respectively. Despite the low growth temperature used, titanium-interdiffusion is observed over 5–6 unit cells (1.4–1.7 nm) near the interface. The extent of the interdiffusion is consistent with the degraded MIT observed in the 1.5 nm thick films arising from an extrinsic origin, i.e., interdiffusion. Ti-doping has been observed to depress $\Delta R/R$ in $(Ti,V)O_2$ single crystal[26,27] and polycrystalline samples.[28] Ti-doping has also been observed to make the metallic state above T_c semiconducting (a negative R vs. T slope);[26,27] indeed, such behavior is seen in the 1.5 nm thick VO_2 films, where the transport is dominated by the interdiffused region. Analysis of the V-$L_{2,3}$ also suggested a slight reduction in the vanadium valence in the interfacial region.[25]

In summary, we have developed an alternative growth method for the epitaxial growth of VO_2 thin films by MBE. Films grown by this technique show reproducible MITs with $\Delta R/R = 10^3$ for VO_2 thicknesses down to 3 nm. The three-dimensional growth mode, combined with interdiffusion with the substrate, limits the achievement of a sharp MIT for thinner films using this technique. The development of other substrates for VO_2 growth with higher surface energy and less prone to interdiffusion than TiO_2 would be an important step on the road to the electric-field control of the MIT in ultra-thin VO_2 films using solid high-K dielectrics.

[1]M. Nakano, K. Shibuya, D. Okuyama, T. Hatano, S. Ono, M. Kawasaki, Y. Iwasa, and Y. Tokura, Nature **487**, 459 (2012).
[2]J. Jeong, N. Aetukuri, T. Graf, T. D. Schladt, M. G. Samant, and S. S. P. Parkin, Science **339**, 1402 (2013).
[3]C. H. Ahn, J.-M. Triscone, and J. Mannhart, Nature **424**, 1015 (2003).
[4]L. A. Ladd and W. Paul, Solid State Commun. **7**, 425 (1969).
[5]C. Ko, Z. Yang, and S. Ramanathan, ACS Appl. Mater. Interfaces **3**, 3396 (2011).
[6]R. M. Bowman and J. M. Gregg, J. Mater. Sci.: Mater. Electron. **9**, 187 (1988).
[7]A. Zimmers, L. Aigouy, M. Mortier, A. Sharoni, S. Wang, K. West, J. Ramirez, and I. Schuller, Phys. Rev. Lett. **110**, 056601 (2013).
[8]K. Martens, N. Aetukuri, J. Jeong, M. G. Samant, and S. S. P. Parkin, Appl. Phys. Lett. **104**, 081918 (2014).
[9]Our analysis criteria[10] yield $\Delta R/R$ of $10^{3.2}$ from data extraction, which is comparable to the $\Delta R/R$ of $10^{3.1}$ from the 10 nm thick VO_2 films reported here. See supplementary Figure S4.[29]
[10]J. W. Tashman, J. H. Lee, H. Paik, J. A. Moyer, R. Misra, J. A. Mundy, T. Spila, T. A. Merz, J. Schubert, D. A. Muller, P. Schiffer, and D. G. Schlom, Appl. Phys. Lett. **104**, 063104 (2014).
[11]Z. Yang, C. Ko, V. Balakrishnan, G. Gopalakrishnan, and S. Ramanathan, Phys. Rev. B **82**, 205101 (2010).
[12]A. Mansingh and R. Singh, Phys. Status Solidi A **49**, 773 (1978).
[13]W. Rosevear and W. Paul, Phys. Rev. B **7**, 2109 (1973).
[14]J. Wei, H. Ji, W. Guo, A. H. Nevidomskyy, and D. Natelson, Nat. Nanotechnol. **7**, 357 (2012).
[15]Calculating the film thicknesses by dividing the RBS areal density (atoms/area) by the film density (atoms/volume) calculated from the measured a-axis and c-axis lengths (Fig. 2(d)) is also consistent with the thicknesses given in Table I as the uncertainty in thickness is dominated by the uncertainty in the RBS areal density, not the film density. For this calculation, films thinner than 10 nm were assumed to be commensurate.
[16]CrysTec, GmbH, Berlin, Germany, Floating-zone grown crystal.
[17]Y. Yamamoto, K. Nakajima, T. Ohsawa, Y. Matsumoto, and H. Koinuma, Jpn. J. Appl. Phys. Part 2 **44**, L511 (2005).
[18]M. Ramamoorthy, D. Vanderbilt, and R. King-Smith, Phys. Rev. B **49**, 16721 (1994).
[19]J. B. Nelson and D. P. Riley, Proc. Phys. Soc. **57**, 160 (1945).
[20]Y. Gu, J. Cao, J. Wu, and L. Q. Chen, J. Appl. Phys. **108**, 083517 (2010).
[21]Y. Muraoka and Z. Hiroi, Appl. Phys. Lett. **80**, 583 (2002).
[22]K. Nagashima, T. Yanagida, H. Tanaka, and T. Kawai, Phys. Rev. B **74**, 172106 (2006).
[23]M. D. Biegalski, D. D. Fong, J. A. Eastman, P. H. Fuoss, S. K. Streiffer, T. Heeg, J. Schubert, W. Tian, C. T. Nelson, X. Q. Pan, M. E. Hawley, M. Bernhagen, P. Reiche, R. Uecker, S. Trolier-McKinstry, and D. G. Schlom, J. Appl. Phys. **104**, 114109 (2008).
[24]Y. Muraoka, K. Saeki, R. Eguchi, T. Wakita, M. Hirai, T. Yokoya, and S. Shin, J. Appl. Phys. **109**, 043702 (2011).
[25]L. F. Kourkoutis, Y. Hotta, T. Susaki, H. Y. Hwang, and D. A. Muller, Phys. Rev. Lett. **97**, 256803 (2006).
[26]J. B. MacChesney and H. J. Guggenheim, J. Phys. Chem. Solids **30**, 225 (1969).
[27]T. Horlin, T. Niklewski, and M. Nygren, Acta Chem. Scand., Ser. A **30**, 619 (1976).
[28]W. Rüdorff, G. Walter, and J. Stadler, Z. Anorg. Allg. Chem. **297**, 1 (1958).
[29]See supplementary material at http://dx.doi.org/10.1063/1.4932123 for additional characterization of the TiO_2 substrates and VO_2 films leading to the optimized film growth conditions reported in this Letter.